Layered Graphene Oxide Nanostructures with Sandwiched Conducting Polymers as Supercapacitor Electrodes

ARTICLE *in* LANGMUIR · OCTOBER 2010

Impact Factor: 4.46 · DOI: 10.1021/la103413s · Source: PubMed

4 AUTHORS, INCLUDING:

Lili Zhang
Institute of Chemical and Engineering Sciences
59 PUBLICATIONS **5,388** CITATIONS

SEE PROFILE

XS Zhao
University of Queensland
310 PUBLICATIONS **14,112** CITATIONS

SEE PROFILE

Langmuir
Article
pubs.acs.org/Langmuir

Layered Graphene Oxide Nanostructures with Sandwiched Conducting Polymers as Supercapacitor Electrodes

Li Li Zhang, Shanyu Zhao, Xiao Ning Tian, and X. S. Zhao*

Department of Chemical and Biomolecular Engineering, National University of Singapore, 4 Engineering Drive 4, Singapore 117576

Received August 29, 2010. Revised Manuscript Received September 30, 2010

We demonstrate a general approach to the preparation of layered graphene oxide structures with sandwiched conducting polymers of different morphologies. The approach is conceptualized on the basis of the electrostatic interactions between negatively charged graphene oxide sheets and positively charged surfactant micelles. A graphene oxide−polypyrrole composite prepared from this approach exhibited an excellent electrocapacitive performance with a high specific capacitance over 500 F g^{-1}. Good rate performance and cycle ability were realized by the composite electrode. The simple method described here opens up a generalized route to making a wide range of graphene oxide-based and graphene-based composite materials for applications beyond electrochemical energy storage.

Introduction

Conducting polymers have been shown as promising electrode materials because of their high conductivity and fast redox activity.[1,2] However, the rapid degradation due to swelling and shrinkage of the polymer can lead to a poor cycle stability. One way to overcome this drawback is to support the conducting polymer on a carbon-based material.[3,4] In this respect, various carbon materials, such as activated carbons (ACs),[5] carbon monolith,[6] templated porous carbons,[4] and carbon nanotubes (CNTs),[7] have been employed to making the composite materials. An improvement on stability has been observed because of the excellent chemical and mechanical stability of the carbon materials. However, the total capacitance values are usually limited by the microstructures of the carbon. In addition, the use of expensive CNTs as a substrate is not cost-effective.

Recently, graphene oxide (GO) has been demonstrated to be a good filler for polymer nanocomposites.[8] GO is a promising starting material as it can be prepared in large scales from graphite,[9] and it is an attractive precursor for the production of functional composite materials because of its easy processability in solution and rich colloidal properties. In our previous work, we have shown that a GO−conducting polymer composite displayed unique electrochemical properties when used as supercapacitor electrodes.[10]

Herein, we demonstrate a new approach to the preparation of conducting polymer−pillared GO sheets as illustrated in Scheme 1.

Scheme 1. Schematic Illustration of the Formation Process of GOPPy Composite

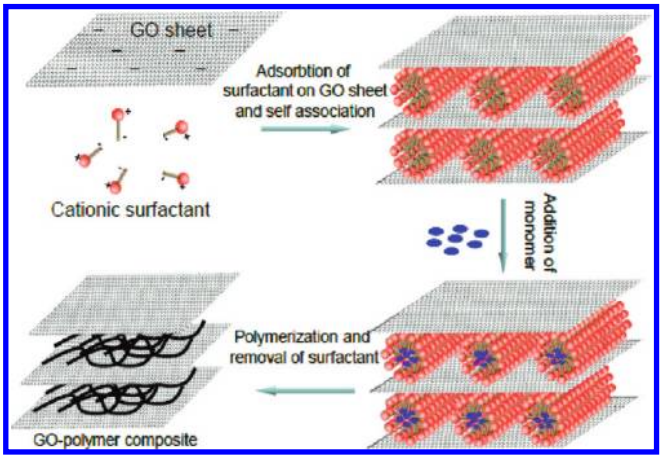

The approach is conceptualized on the basis of the electrostatic interactions between negatively charged GO sheets[11] and positively charged surfactant micelles. When a cationic surfactant solution of concentration well above its critical micellization concentration (cmc) is combined with a GO dispersion, the surfactant micelles will electrostatically adsorb on the surfaces of the GO sheets, forming a GO−surfactant multilayer structure with the surfactant micelles sandwiched between the GO sheets. When a conducting polymer monomer is added, the monomer will be predominately solubilized in the hydrophobic cores of the surfactant micelles. Upon adding an initiator, polymerization will also undergo predominately in the micelle cores. Removal of the surfactant by washing leads to a layered GO structure pillared with the conducting polymer. The morphology of the conducting polymer can be controlled by controlling the morphology of the surfactant micelles. Illustrated in Scheme 1 is the preparation of GO sheets pillared by conducting polymer fibers. It becomes obvious that spherical micelles will lead to the formation of conducting polymer spheres.

*Corresponding author. E-mail: chezxs@nus.edu.sg. Fax: 65-67791936.

(1) Roberts, M. E.; Wheeler, D. R.; McKenzie, B. B.; Bunker, B. C. *J. Mater. Chem.* **2009**, *19*, 6977–6979.
(2) Nystrom, G.; Razaq, A.; Stromme, M.; Nyholm, L.; Mihranyan, A. *Nano Lett.* **2009**, *9*, 3635–3639.
(3) Zhang, L. L.; Li, S.; Zhang, J.; Guo, P.; Zheng, J.; Zhao, X. S. *Chem. Mater.* **2010**, *22*, 1195–1202.
(4) Wang, Y.-G.; Li, H.-Q.; Xia, Y.-Y. *Adv. Mater.* **2006**, *18*, 2619–2623.
(5) Bleda-Martinez, M. J.; Peng, C.; Zhang, S.; Chen, G. Z.; Morallon, E.; Cazorla-Amoros, D. *J. Electrochem. Soc.* **2008**, *155*, A672–A678.
(6) Fan, L. Z.; Hu, Y. S.; Maier, J.; Adelhelm, P.; Smarsly, B.; Antonietti, M. *Adv. Funct. Mater.* **2007**, *17*, 3083–3087.
(7) Hughes, M.; P. S., M. S.; Renouf, A. C.; Singh, C.; Chen, G. Z.; Fray, D. J.; Windle, A. H. *Adv. Mater.* **2002**, *14*, 382–385.
(8) Cassagneau, T.; Guerin, F.; Fendler, J. H. *Langmuir* **2000**, *16*, 7318–7324.
(9) Li, D.; Kaner, R. B. *Science* **2008**, *320*, 1170–1171.
(10) Zhang, K.; Zhang, L. L.; Zhao, X. S.; Wu, J. *Chem. Mater.* **2010**, *22*, 1392–1401.
(11) Li, D.; Muller, M. B.; Gilje, S.; Kaner, R. B.; Wallace, G. G. *Nature Nanotechnol.* **2008**, *3*, 101–105.

Such a GO−conducting polymer composite material possesses the unique properties of both the GO and the conducting polymer, such as good mechanical strength because of the carbon matrix, excellent electrical conductivity due to the conducting polymer and the GO if it is reduced to graphene or reduced graphene oxide, and pseudocapacitance due to the conducting polymer, thus holding a great promise for hybrid supercapacitors. Indeed, our experimental data revealed that the nanostructured composite material displayed a significantly higher capacitance than commercial supercapacitor electrodes (typically less than 200 F g^{-1}).[12−14] For example, a GO−polypyrrole composite prepared from this approach exhibited a high specific capacitance of 510 F g^{-1} with good rate capability and cycle stability. The simple method described in this work opens up a generalized route to making a wide range of GO-based composite materials for applications like energy storage and conversion.

Experimental Section

Preparation of GO and Reduced GO (GOR). The GO dispersion was prepared by simple sonication of graphite oxide that was obtained from natural graphite using a modified Hummers method.[10,15] Graphite (5 g) and $NaNO_3$ (2.5 g) were mixed with a 95% H_2SO_4 (120 mL) in a 500 mL flask. The mixture was stirred for 30 min in an ice bath. Under vigorous stirring, 15 g of $KMnO_4$ was added to the suspension. The rate of addition was controlled to keep the reaction temperature lower than 20 °C. The ice bath was then removed, and the mixture was stirred at room temperature overnight. As the reaction progressed, the mixture gradually became pasty, and the color turned into light brownish. Afterward, 150 mL of deionized (DI) H_2O was slowly added to the pasty mixture still under vigorous agitation. The reaction temperature was observed to rapidly increase to 98 °C with effervescence, and the color changed to yellow. The diluted suspension was stirred for 1 day. Then, 50 mL of 30% H_2O_2 was added to the mixture. To purify, the mixture was washed with 5% of HCl and then DI H_2O for several times to obtain the graphite oxide sample. The final GO dispersion was prepared by sonication of graphite oxide. The reduction of GO was carried out using the hydrazine reduction method as described elsewhere.[16]

Preparation of GO−Conducting Polymer Composites. As shown in Scheme 1, the morphology of the conducting polymer between GO sheets can be controlled by controlling the shape of the surfactant micelles. Two GO−conducting polymer composite samples with fibrous and spherical morphologies of the conducting polymer were prepared. For the preparation of conducting polymer−fiber-pillared GO sheets (this sample is denoted as GOPPy-F), 3.6 g of cetyltrimethylammonium bromide (CTAB, 99% Aldrich) dissolved in 40 mL of 1 M HNO_3 solution was added to 0.05 g of GO dispersion (10 mg mL^{-1}) under stirring. Then, 0.4 g of pyrrole (98%, Aldrich) was added to the system at 10 °C. After stirring for 60 min, 20 mL of ammonium persulfate (APS, molar ratio of APS to pyrrole was 1:1) was added to initiate the polymerization. After 180 min, the solid product was collected by filtration and washed with DI water and finally with ethanol, followed by vacuum drying at 60 °C for 1 day. For the preparation of conducting polymer−sphere-pillared GO sheets (this sample is denoted as GOPPy-S), 1 g of decyl alcohol (99%, Aldrich) was mixed with 30 mL of DI water under stirring. After 10 min, the mixture was added to 0.1 g of GO dispersion (10 mg mL^{-1}). Then, 1.5 g of dodecyltrimethylammonium bromide (DTAB, 99%, Aldrich) was added, and the temperature was maintained at 1 °C. After stirring for 20 min, the mixture was transferred to an ultrasonicator (Elma Transsonic T460/H of capacity 2.5 L and frequency of 35 kHz). Subsequently, 0.8 g of pyrrol was added dropwise. Polymerization was initiated by adding 2 g of $FeCl_3$ (99%, Aldrich). After ultrasonication for 60 min, the solid product was collected by filtration and washed with DI water and finally ethanol, followed by vacuum drying at 60 °C for 1 day.

Preparation of Other Samples for Comparison. A pure PPy fiber sample was prepared similarly to that of GOPPy-F but without the presence of the GO dispersion. This sample is denoted as PPy-F. A pure PPy sphere sample was also prepared similarly to that of sample GOPPy-S but without the presence of the GO dispersion. This sample is denoted as PPy-S. To examine the role of surfactant micelles in determining the morphology of the composite, another sample was prepared under the similar experimental conditions of sample GOPPy-F but without the presence of surfactant CTAB. This sample is denoted as GO-PPy.

Characterization. The microscopic feature of the samples was observed on a field-emission scanning electron microscope (FESEM) (JSM 6700F, JEOL Japan) operated at 10 kV and a transmission electron microscope (TEM) (JEM 2010, JEOL, Japan) operated at 200 kV. Fourier-transform infrared (FT-IR) spectra were acquired using the attenuated total reflectance (ATR) technique on an IRPrestige-21 (Shimadzu, Japan). X-ray diffraction (XRD) patterns were collected on an XRD-6000 (Shimadzu, Japan) with Cu Kα radiation with $\lambda = 1.5406$ Å. X-ray photoelectron spectroscopy (XPS) measurements were carried out on an AXIS HSI 165 spectrometer (Kratos Analytical) using a monochromatized Al Kα X-ray source (1486.71 eV).

Electrochemical Measurement. A three-electrode cell system was used to evaluate the electrochemical performance using both the cyclic voltammetry (CV) and galvanostatic charge−discharge techniques on an Autolab PGSTAT302N at room temperature. A 2 M H_2SO_4 aqueous solution was employed as the electrolyte. A platinum sheet and a saturated Ag/AgCl electrode were used as the counter and the reference electrodes, respectively. The working electrode was prepared by casting a Nafion-impregnated sample onto a glassy carbon electrode with diameter of 5 mm.[10] Typically, 5 mg of composite material was dispersed in 1 mL of ethanol solution containing 5 μL of Nafion solution (5 wt % in water) by sonication for 20 min. This sample (40 μL) was then dropped onto the glassy carbon electrode and dried in an oven before the electrochemical test. The mass loading of the sample on the glassy carbon electrode is 1 mg cm^{-2}.

The specific gravimetric capacitance (C in F g^{-1}) was obtained from the discharge process according to the following equation:[17,18]

$$C = \frac{I\Delta t}{\Delta V m} \quad (1)$$

where I is the current loaded (A), Δt is the discharge time (s), ΔV is the potential change during discharge process, and m is the mass of active material in a single electrode (g).

Results and Discussion

Zeta Potential Analysis. To prove our conceptualized approach, the surface charge of the GO dispersion before and after adding the surfactant CTAB solution was measured using the zeta potential technique. The zeta potential profiles shown in Figure 1 revealed that the GO dispersion was negatively charged over a wide pH range, which is due to the ionization of functional groups on the GO surface, such as hydroxyl and carboxylic acid groups. This observation is consistent with that reported in the literature.[11] After adding surfactant CTAB, the GO dispersion became almost completely negatively charged in the pH range studied in this work.

(12) Zhang, L. L.; Zhao, X. S. *Chem. Soc. Rev.* **2009**, *38*, 2520–2531.
(13) Naoi, K.; Simon, P. *Electrochem. Soc. Interface* **2008**, *17*, 34–37.
(14) Simon, P.; Burke, P. *Electrochem. Soc. Interface* **2008**, *17*, 38–43.
(15) Hummers, W. S.; Offeman, R. E. *J. Am. Chem. Soc.* **1958**, *80*, 1339–1339.
(16) Stankovich, S.; Dikin, D. A.; Piner, R. D.; Kohlhaas, K. A.; Kleinhammes, A.; Jia, Y.; Wu, Y.; Nguyen, S. T.; Ruoff, R. S. *Carbon* **2007**, *45*, 1558–1565.
(17) Seredych, M.; Hulicova-Jurcakova, D.; Lu, G. Q.; Bandosz, T. J. *Carbon* **2008**, *46*, 1475–1488.
(18) Hulicova, D.; Kodama, M.; Hatori, H. *Chem. Mater.* **2006**, *18*, 2318–2326.

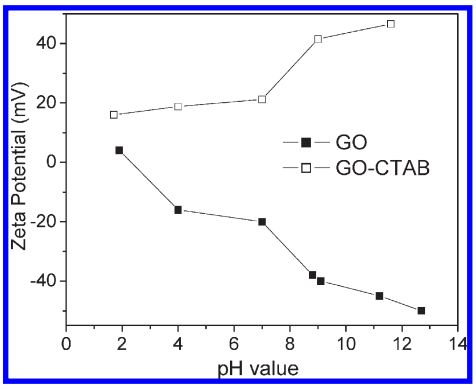

Figure 1. Zeta potential profiles of a graphene oxide dispersion before (GO) and after adding surfactant CTAB (GO−CTAB).

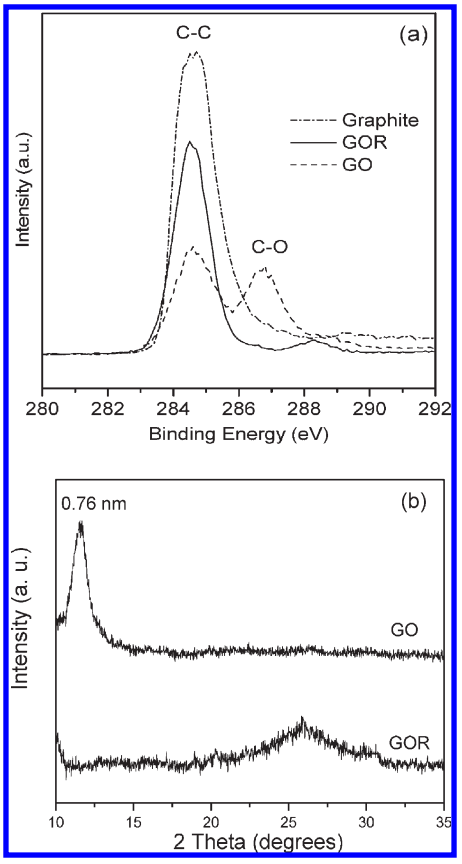

Figure 2. (a) C 1s XPS spectra of GO, GOR, and pristine graphite. (b) XRD patterns of GO and GOR.

The zeta potential data demonstrated that surfactant CTAB micelles indeed adsorbed on the GO sheets to result in a reverse of the surface charge.

Physical and Chemical Properties of the Samples. The XPS and XRD data of samples GO and GOR are shown in Figure 2. The C 1s XPS spectrum shown in Figure 2a clearly indicated a considerable degree of oxidation of graphite upon chemical exfoliation. The two prominent peaks seen on sample GO revealed the presence of a large amount of functional groups on the surface of the GO.[19] Upon reduction, the C−O bond diminished while the C═C bond dominated as evidenced by the presence of only one peak at about 284.5 eV.[19] The small peak at about 288.5 eV indicated there was a small amount of carboxyl group in sample GOR.

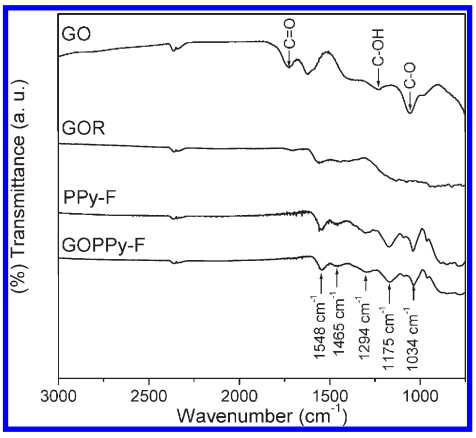

Figure 3. FTIR spectra of sample GO, GOR, PPy-F, and GOPPy-F.

The XRD patterns shown in Figure 2b exhibited one sharp peak centered at $2\theta = 11.6°$ for the stacked GO sample after the drying process. This is correlated to a layer-to-layer distance (d-spacing) of 0.76 nm. After hydrazine reduction (sample GOR), this peak disappeared and a broad peak centered at $2\theta = 25.8°$ emerged, indicating a successful exfoliation and a loosely packed graphene sheets in GOR.[20]

The presence of the surface functional groups on the GO sheets was further confirmed by the FTIR data shown in Figure 3 because the main absorption bands can be assigned to C═O, C−OH, and C−O vibrations.[11,21] These absorption bands, however, are hardly seen on the reduced GO sample (GOR), indicating the functional groups had been essentially removed by hydrazine. There are a number of absorption bands that can be seen on sample PPy-F. The peaks at 1548 and 1465 cm^{-1} are due to the fundamental stretching vibrations of pyrrole rings.[22] The bands at 1294 and 1034 cm^{-1} are due to the C−N stretching and C−H deformation vibrations, respectively. The strong absorption band at about 1175 cm^{-1} indicates that the PPy is doped.[22,23] All of the above peaks can be seen from sample GOPPy-F, showing the composite sample contained PPy. No vibration signals due to methylene appearing at 2848 and 2929 cm^{-1} are seen, indicating that CTAB had been completely removed.[23]

Morphological Properties of the Samples. The layered structure of the solid GO sample with stacked GO sheets can be seen from the FESEM image shown in Figure 4a. The TEM image (Figure 4b) showed a typical single layer GO sheet with a lateral dimension of several micrometers. As for the GOPPy-F composite, a flat and layered structure can be clearly seen from Figure 4c with PPy fibers either sandwiched between GO sheets or on the GO surfaces. The TEM image (Figure 4d) also confirmed the presence of PPy fibers sandwiched between the GO sheets. For the pure PPy sample (PPy-F) prepared in the absence of a GO dispersion, only random PPy fibers are seen as revealed by both the FESEM (Figure 4e) and TEM (Figure 4f) images.

In this preparation method, surfactant plays a paramount role in forming such a conducting polymer−pillared GO composite structure. In our experiment, a sample was prepared under

(19) Gao, W.; Alemany, L. B.; Ci, L.; Ajayan, P. M. *Nature Chem.* **2009**, *1*, 403–408.
(20) Cote, L. J.; Cruz-Silva, R.; Huang, J. *J. Am. Chem. Soc.* **2009**, *131*, 11027–11032.
(21) Li, X.; Zhang, G.; Bai, X.; Sun, X.; Wang, X.; Wang, E.; Dai, H. *Nature Nanotechnol.* **2008**, *3*, 538–542.
(22) Wei, Z.; Zhang, L.; Yu, M.; Yang, Y.; Wan, M. *Adv. Mater.* **2003**, *15*, 1382–1385.
(23) Zhong, W.; Liu, S.; Chen, X.; Wang, Y.; Yang, W. *Macromolecules* **2006**, *39*, 3224–3230.

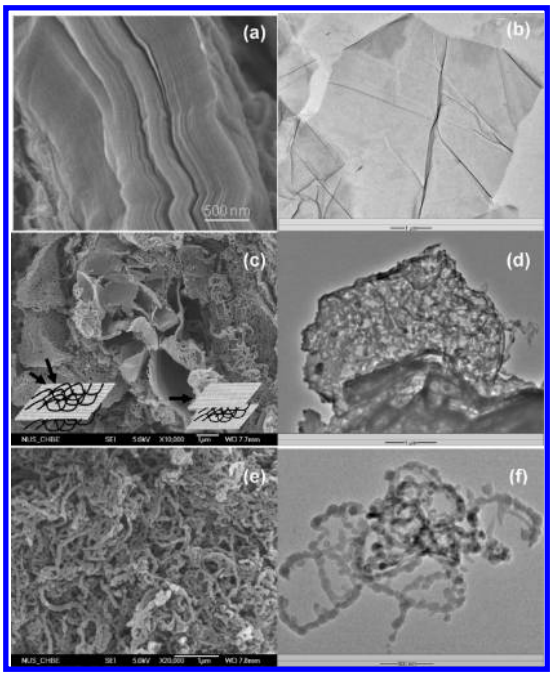

Figure 4. FESEM images of (a) GO, (c) GOPPy-F, and (e) PPy-F and TEM images of (b) GO, (d) GOPPy-F, and (f) PPy-F.

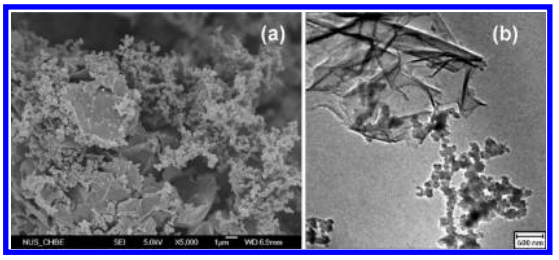

Figure 5. (a) FESEM image and (b) TEM image of sample GO-PPy.

otherwise the same experimental conditions to that of sample GOPPy-F, except for the absence of surfactant CTAB. The sample thus prepared is denoted as GO-PPy. Figure 5 showed the FESEM and TEM images of sample GO-PPy. It can be seen that in the absence of surfactant CTAB no layered or flat composite structure was obtained. Instead, only separate PPy particles and GO sheets were obtained. This experimental data strongly support our conceptualized preparation route in which the surfactant micelles interact with the GO sheets to form a GO−surfactant multilayer structure, leading to the formation of a layered GO structure with conducting polymer sandwiched between GO sheets as pillars.

In addition, the morphology of the conducting polymer can be controlled by varying the surfactant and adding a coadsorbing molecule.[24] For example, we have also succeeded in synthesizing a layered GO structure pillared by PPy spheres (sample GOPPy-S) in the presence of surfactant dodecyltrimethylammonium bromide (DTAB) and solvent 1-decanol. In this case, spherical micelles directed the formation of the PPy spheres. The use of 1-decanol was to enhance the size uniformity and stability of micelles.[25] Figure 6a,b shows the FESEM images of sample GOPPy-S at different magnifications. It was revealed that PPy spheres instead of PPy fibers were sandwiched between GO

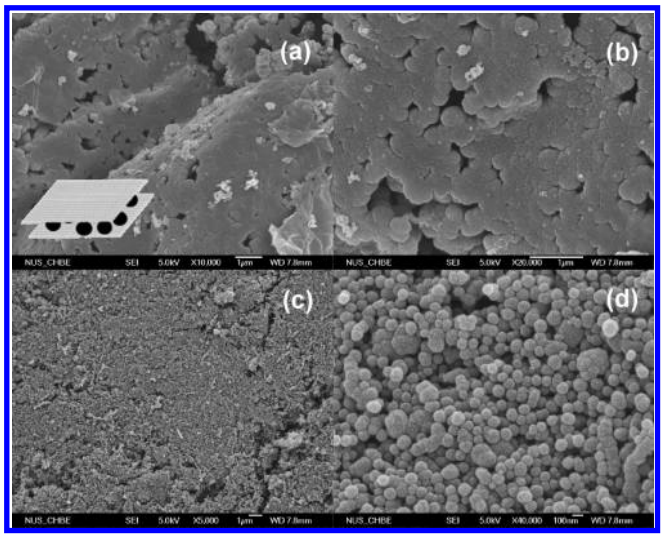

Figure 6. FESEM images of (a, b) GOPPy-S and (c, d) PPy-S.

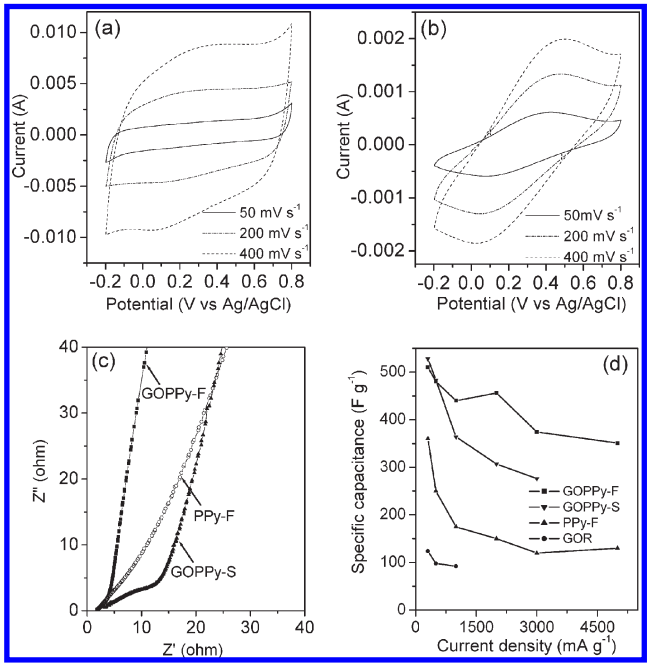

Figure 7. CV profiles of (a) GOPPy-F and (b) PPy-F measured at different sweep rates. (c) Nyquist plots of GOPPy-F and PPy-F. (d) Specific capacitance as a function of current density.

sheets. In the case of the pure PPy spheres sample (PPy-S) prepared without the presence of a GO dispersion, only random PPy spheres without sheetlike structure were observed as shown in Figure 6c,d at different magnifications.

Electrochemical Properties of the Samples. The electrochemical properties of samples are compared in Figure 7. The specific gravimetric capacitances of samples under different current loads are summarized in Table 1. The cyclic voltammetry (CV) curves of sample GOPPy-F (Figure 7a) exhibited a rectangular shape at sweep rates ranging from 50 to 400 mV s^{-1}. In contrast, the CV curves for the pure PPy fiber sample (Figure 7b) were distorted. The above results demonstrate a better charge propagation behavior and ion response of sample GOPPy-F than sample PPy-F.[26] The significantly improved ion transport

(24) Carswell, A. D. W.; O'Rea, E. A.; Grady, B. P. *J. Am. Chem. Soc.* **2003**, *125*, 14793–14800.
(25) Wang, Y.; Su, F.; Wood, C. D.; Lee, J. Y.; Zhao, X. S. *Ind. Eng. Chem. Res.* **2008**, *47*, 2294–2300.
(26) Wang, D.; Li, F.; Liu, M.; Lu, G.; Cheng, H. M. *Angew. Chem., Int. Ed.* **2008**, *47*, 373–376.

Table 1. Specific Gravimetric Capacitance of Various Electrodes at Different Current Densities

samples	0.3 A g^{-1}	0.5 A g^{-1}	1 A g^{-1}	2 A g^{-1}	3 A g^{-1}	5 A g^{-1}
GOR	124	98	92			
GOPPy-F	510	480	440	456	374	351
PPy-F	360	250	175	150	120	130
GOPPy-S	528	483	364	307	276	255

behavior of sample GOPPy-F was further characterized using the electrochemical impedance spectroscopy (EIS) technique with a frequency range of 0.1 Hz−10 kHz. EIS is a powerful technique complementary to galvanostatic cycling measurement that provides more information on the electrochemical frequency behavior of the system. The EIS data were analyzed using Nyquist plots and are presented in Figure 7c. The negligible high-frequency resistor−capacitor (RC) loops or semicircles for both samples GOPPy-F and the PPy-F indicate a good electrode contact.[27] The 45° sloped portion of the Nyquist plots, the so-called Warburg resistance,[28] is a result of the frequency dependence of ion transport in the electrolyte. The smaller Warburg region of sample GOPPy-F than that of sample PPy-F indicates a lower ion diffusion resistance and less obstruction of the ion movement, thus better charge propagation and ion response of sample GOPPy-F than sample PPy-F.

The excellent capacitive performance of the composite electrodes can be clearly seen from Figure 7d. Compared to sample GOR, the significantly improved capacitance of sample GOPPy-F is attributed to the effective pseudocapacitive contribution of the PPy fibers in the composite electrode. While the pure PPy fiber sample exhibited a high capacitance value (360 F g^{-1}, see Table 1), its rate performance was poor as the capacitance was below 150 F g^{-1} when the current density was increased to 5 A g^{-1}. On contrast, a very high specific capacitance of 510 F g^{-1} was obtained on sample GOPPy-F and a high capacitance retention ratio (about 70%) was observed when the current density was increased by 17 times. It is interesting to note that sample GOPPy-S performed similarly to that of GOPPy-F at low current density. However, when the current density increased, sample GOPPy-S performed worse than that of GOPPy-F. Considering that the weight percentages of PPy in both composite materials are similar, the difference between the capacitive performance of the two composite electrode materials is due to the different morphology, which resulted in different ion transport resistance. This can be seen from the Nyquist plots in Figure 7c. A larger Warburg region of sample GOPPy-S than that of GOPPy-F indicated a higher ion diffusion resistance of the former one, which resulted in poorer capacitive performance at high current density. However, when the current density is low, there is enough response time for the electrolyte ions to reach the active surface of both samples. Hence, similar performance is observed for GOPPy-S and GOPPy-F. Therefore, our experimental results implied the morphology of the conducting polymer played a very important role in the electrochemical performance. PPy with fiberlike structure in the composite material is beneficial for high-rate electrode material.

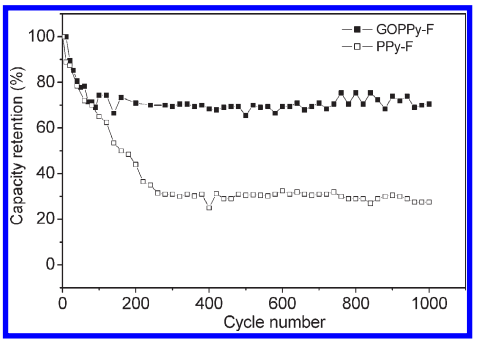

Figure 8. Cycling performance of the electrode materials GOPPy-F and PPy-F under a current density of 5 A g^{-1}.

The advantage of the composite electrode GOPPy-F over the pure conducing polymer is clearly demonstrated. The support carbon matrix GO allowed the deposition of the conducting polymer on both surfaces of the GO sheets. In addition, the strong attachment between the carbon matrix and PPy enhanced the mechanical strength of the composite materials, which is highly favorable for long charge−discharge cycle ability. Indeed, Figure 8 shows the electrochemical stability of the composite electrode GOPPy-F and the pure PPy-F at a current density of 5 A g^{-1}. It is seen that over 70% of the original capacitance was retained for the composite electrode GOPPy-F after 1000 cycles, while only 30% was retained for the pure PPy-F electrode, indicating a much better cycle ability of the composite material than the pure polymer electrode.

Conclusions

In summary, we have demonstrated an approach to the preparation of conducting polymer−pillared graphene oxide sheets with excellent electrocapacitive properties. Such nanostructured composites embrace the unique properties of both graphene oxide and conducting polymers. The advantages of the composite materials include the following: (1) the exfoliated GO sheets dispersed in solution provide large accessible surface for the attachment of the conducting polymer on both sides; (2) the three-dimensional layered structure would enhance the mechanical strength of the composite and stabilize the polymers during the charge−discharge process; (3) the GO nanostructure with conducting polymer pillars effectively reduces the dynamic resistance of electrolyte ions; and (4) the readily accessible conducting polymers contribute pseudocapacitance to the overall energy storage to a great extent. Considering the simple method and wide-range potential applications of the composite structures, the concept introduced in this work can be extended for making other graphene-based architectures for applications beyond supercapacitors.

Acknowledgment. Financial support from Ministry of Education of Singapore (MOE2008-T2-1-004) is greatly appreciated.

(27) Portet, C.; Lillo-Rodenas, M. A.; Linares-Solano, A.; Gogotsi, Y. *Phys. Chem. Chem. Phys.* **2009**, *11*, 4943–4945.
(28) Kotz, R.; Carlen, M. *Electrochim. Acta* **2000**, *45*, 2483–2498.